Journal of Materials Chemistry

Cite this: *J. Mater. Chem.*, 2012, **22**, 22998

www.rsc.org/materials

PAPER

Efficient solid-state white light-emitting electrochemical cells based on phosphorescent sensitization

Hai-Ching Su,*[a] Hsiao-Fan Chen,[b] Po-Hsien Chen,[a] Shih-Wei Lin,[b] Chih-Teng Liao[a] and Ken-Tsung Wong[b]

Received 14th August 2012, Accepted 13th September 2012
DOI: 10.1039/c2jm35483g

Efficient phosphorescent sensitized white light-emitting electrochemical cells (LECs) based on a blue-emitting phosphorescent cationic transition metal complex (CTMC) doped with a red-emitting fluorescent dye are demonstrated. Blue phosphorescence and phosphorescence-sensitized red fluorescence contribute to white emission. Furthermore, the microcavity effect of the device structure is utilized to suppress the green part of the electroluminescence (EL) spectrum of the blue-emitting phosphorescent metal complex (**1**) *via* destructive interference. Hence, more saturated blue EL emission can be obtained. When combined with saturated red emission, white EL emission with Commission Internationale de l'Eclairage coordinates approaching (0.33, 0.33) can be obtained without the need for saturated deep-blue emitting CTMCs. Peak external quantum efficiency and power efficiency of the phosphorescence sensitized white LECs are up to 7.9% and 15.6 lm W^{-1}, respectively. These efficiencies are among the highest reported for white LECs and reveal that phosphorescent sensitization is useful for improving device efficiencies of white LECs.

Introduction

White organic light-emitting diodes (OLEDs) have attracted intense attention due to their potential applications in flat-panel displays and solid-state lighting.[1] Compared with conventional OLEDs, solid-state light-emitting electrochemical cells (LECs)[2] possess several promising advantages. LECs generally require only a single emissive layer, which can be easily processed from solutions, and can conveniently use air-stable electrodes. The emissive layers of LECs contain mobile ions, which can drift toward electrodes at an applied bias. The spatially separated ions induce electrochemical doping (oxidation and reduction) of the emissive materials near the electrodes, *i.e.* p-type doping near the anode and n-type doping near the cathode.[2] The doped regions induce ohmic contacts with the electrodes and consequently facilitate the injection of both holes and electrons, which recombine at the junction between p- and n-type regions. As a result, a single-layered LEC device can be operated at very low voltages (close to E_g/e, where E_g is the energy gap of the emissive material and e is the elementary charge) with balanced carrier injection, giving high power efficiencies. Furthermore, air-stable metals can be used since carrier injection in LECs is relatively insensitive to work functions of electrodes.

Several studies of fluorescent solid-state white LECs based on conjugated polymers have been reported.[3–5] However, moderate efficiencies of polymer white LECs showed that the fluorescent nature of conjugated polymers limits the eventual electroluminescence (EL) efficiency due to the spin statistics. To improve device efficiencies, phosphorescent cationic transition metal complexes (CTMCs) have been intensively studied for their use in solid-state LECs.[6–32] Furthermore, compared with conventional polymer LECs, no ion-conducting material (*e.g.* poly(ethylene oxide), PEO) is needed in CTMC-based LECs since CTMCs are intrinsically ionic. By employing a blue-emitting host and a red-emitting guest, solid-state white LECs based on CTMCs have been demonstrated to exhibit efficient white EL emission[18,20,21,24] and an external quantum efficiency (EQE) up to 7.4% was achieved.[24] Further improvement in device efficiency would be impeded by low photoluminescence quantum yields (PLQYs) of the red-emitting CTMCs (<0.2 even in dilute solutions) used in CTMC-based white LECs.[18,20] Recently, fluorescent LECs based on phosphorescent sensitization[33] have been demonstrated to be an alternative way to reach efficiencies similar to phosphorescent LECs.[23,26] In phosphorescence sensitized fluorescence, the heavy-metal center of the phosphorescent host mediates rapid inter-system crossing for efficient intramolecular singlet-to-triplet energy transfer, and thus subsequent effective Förster energy transfer[34] from triplet excitons of the phosphorescent host to singlet excitons of the fluorophore guest, harvesting both singlet and triplet excitons in hosts. As a result, device efficiencies of phosphorescence sensitized fluorescent LECs could approach those of phosphorescent LECs. White OLEDs incorporating a blue phosphorescent dye, which acts not only as a phosphorescent sensitizer but also a blue emitter, and a fluorescent red dye have been reported to exhibit efficient white

[a]*Institute of Lighting and Energy Photonics, National Chiao Tung University, Tainan 71150, Taiwan. E-mail: haichingsu@mail.nctu.edu.tw; Fax: +886-6-3032535; Tel: +886-6-3032121-57792*
[b]*Department of Chemistry, National Taiwan University, Taipei 10617, Taiwan*

EL emission.[35] Since various efficient red-emitting fluorescent dyes[36] (PLQYs > 0.9 in dilute solutions) are commercially available, phosphorescent sensitization would also be a feasible way to achieve efficient host–guest white LECs. Despite its practical potential, reports of white LECs based on phosphorescent sensitization would still have been scarce up to now to the best of our knowledge.

In this work, we demonstrate efficient white LECs based on a blue-emitting phosphorescent CTMC as the host and a red-emitting fluorescent dye as the guest. Peak EQE and power efficiency of the phosphorescent sensitized white LECs reach 7.9% and 15.6 lm W^{-1}, respectively. These efficiencies are among the highest reported for white LECs and confirm that phosphorescent sensitization is a useful technique for enhancing device efficiencies of white LECs. Furthermore, the microcavity effect of the device structure is found to alter the output EL spectrum and white EL emission spectra with Commission Internationale de l'Eclairage (CIE) coordinates approaching (0.33, 0.33) can thus be obtained from white LECs without employing saturated deep-blue emitting CTMCs, which have still been scarce up to now.

Results and discussions

Photoluminescent studies

Molecular structures of the CTMC (complex **1**) and the red dye used in this study are shown in Fig. 1. The phosphorescent blue-emitting CTMC $[Ir(dfppz)_2(dtb\text{-}bpy)]^+(PF_6^-)$ (where dfppz is 1-(2,4-difluorophenyl)pyrazole and dtb-bpy is [4,4′-di(*tert*-butyl)-2,2′-bipyridine]) reported previously by Tamayo *et al.*[13] was used as the host material. $[Ir(dfppz)_2(dtb\text{-}bpy)]^+(PF_6^-)$ was synthesized according to the procedures reported in the literature.[13] The fluorescent red dye sulforhodamine 101 (**SR 101**), which has been reported to exhibit a high PLQY up to 0.95 ± 0.02 in solutions,[37] was utilized as the guest material. **SR 101** was purchased from the Acros Organics and was used as received. The PL spectrum of the neat films of complex **1** and absorption/PL spectra of **SR 101** in dilute (10^{-5} M) ethanol solutions are shown in Fig. 2. Neat films of complex **1** exhibit sky-blue phosphorescent PL centered at 490 nm. Highly retained PLQY of complex **1** in neat films (0.75)[24] in comparison with that in dilute solutions (1.00)[24] reveals reduced self-quenching in neat films possibly resulting from the sterically bulky di-*tert*-butyl groups of the bipyridine ligand,[13] suggesting its suitability for use as the emissive host material of white LECs. **SR 101** in ethanol solutions exhibits concentrated red PL spectra centered at 602 nm. It is noted that the absorption spectrum of **SR 101** and the PL spectrum of complex **1** exhibit good spectral overlap (Fig. 2) and thus efficient energy transfer between them would be expected (calculated Förster radius = 4.2 nm). Fig. 3 depicts the PL spectra of thin films of complex **1** containing various concentrations (0.3, 0.5 and 0.8 wt%) of **SR 101**. The excitation wavelength is 365 nm, at which the absorption of complex **1** is much higher than that of **SR 101** at low doping concentrations, minimizing direct absorption of **SR 101** and thus ensuring **SR 101** emission mainly coming from energy transfer. With the increase of the **SR 101** concentration, the relative intensity of the **SR 101** emission with respect to the complex **1** emission is larger due to a relatively higher energy transfer rate at a higher **SR 101** concentration. Measured PLQYs of thin films of complex **1** containing **SR 101** concentrations of 0.3, 0.5 and 0.8 wt% were 0.72, 0.73 and 0.60, respectively. The host–guest samples with relatively lower **SR 101** concentrations (0.3 and 0.5 wt%) show similar PLQYs as compared to neat host films of complex **1** (PLQY = 0.75).[24] It reveals that **SR 101** at low doping concentrations exhibits high PLQYs comparable with those of neat films of complex **1**. Such a PLQY is significantly higher than that of previously used red-emitting CTMCs[18,20] in white LECs and thus it is beneficial in enhancing device efficiencies of white LECs. The reduced PLQY of the samples with a relatively higher **SR 101** concentration (0.8 wt%) would result from the self-quenching effect of **SR 101** molecules. As the **SR 101** concentration increases, the probability of collisions between excited states on **SR 101** also increases and thus the number of radiative excitons decreases, rendering a deteriorated luminescent efficiency.

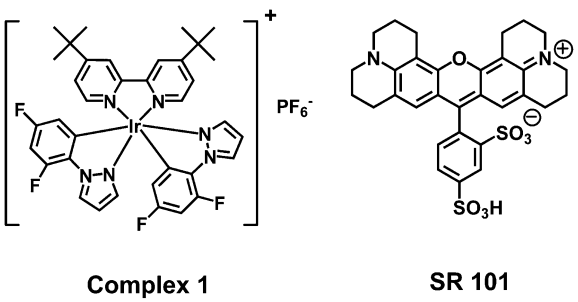

Fig. 1 Molecular structures of complex **1** and the red dye **SR 101**.

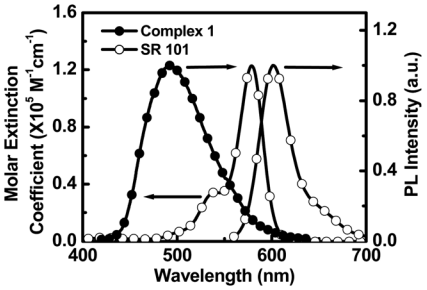

Fig. 2 PL spectra of the neat film of complex **1** and absorption/PL spectra of **SR 101** in ethanol solution (10^{-5} M).

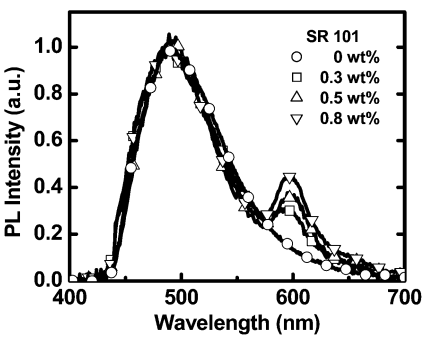

Fig. 3 PL spectra of thin films of complex **1** containing various concentrations of **SR 101**.

EL characteristics of the phosphorescent sensitized white LEC devices

To clarify the EL characteristics of phosphorescent sensitized white LECs, EL data of LECs based on complex **1** doped with various concentrations of **SR 101** were measured and are summarized in Table 1. The white LECs have the structure of glass/indium tin oxide (ITO) (120 nm)/poly(3,4-ethylenedioxythiophene):poly(styrene sulfonate) (PEDOT:PSS) (30 nm)/emissive layer (320 nm)/Ag (100 nm), where the emissive layer contains complex **1** [(80 − x) wt%], **SR 101** (x wt%), and $BMIM^+(PF_6^-)$ (20 wt%) for Device I ($x = 0.3$), Device II ($x = 0.5$) and Device III ($x = 0.8$). The ionic liquid $BMIM^+(PF_6^-)$ of 20 wt% was added to provide additional mobile ions and to shorten the device response time.[12] The EL spectra of Devices I–III at 3.6 and 3.8 V are shown in Fig. 4(a)–(c), respectively. Compared with PL (Fig. 3), the relative intensity of the red emission with respect to the blue emission is larger in EL and slightly increases as the bias decreases for all devices. These results could be understood by energy level alignments of the host and the guest molecules (estimated by cyclic voltammetry) depicted in the inset of Fig. 5.[24] For host–guest LECs, electrochemically doped regions of the emissive layer result in approximate ohmic contact with metal electrodes and consequently facilitate carrier injection into both the host and the guest. Therefore, both exciton formation on the host followed by host–guest energy transfer and direct exciton formation on the guest induced by charge trapping contribute to the guest emission. At lower biases, such energy level alignments (inset of Fig. 5) favor carrier injection and trapping on the smaller-gap guests, resulting in direct exciton formation on the guest (rather than host–guest energy transfer). Hence, slightly larger fractions of guest emission are observed at lower biases. As the bias increases, carrier injection into the host and subsequent host–guest energy transfer would be facilitated, resulting in enhanced host emission. In addition, the device thickness also affects the charge trapping effect. When biased at the same voltage, a lower electric field in a thicker device would also facilitate charge trapping on the guest. However, a higher electric field in a thinner device would lead to direct exciton formation on the host and subsequent host–guest energy transfer. The ratio of the red emission with respect to the blue emission is slightly larger in white LECs with larger **SR 101** concentrations due to two reasons. First, the energy transfer rate between the host and the guest is slightly higher when the **SR 101** concentration increases from 0.3 to 0.8 wt% (Fig. 3). The other reason is that the charge trapping effect due to the host–guest energy level offset (inset of Fig. 5) enhances as the doping concentration increases and thus direct exciton formation on the guest is more significant, resulting in more red emission. The charge trapping effect is confirmed by the doping concentration dependent maximum current density of the white LECs shown in

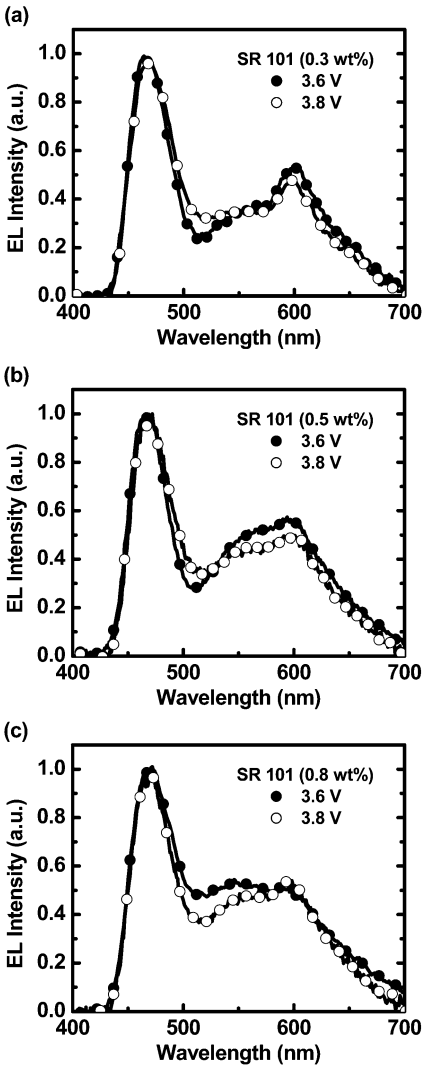

Fig. 4 The EL spectra of the white LECs containing **SR 101** of (a) 0.3, (b) 0.5 and (c) 0.8 wt% at 3.6 and 3.8 V.

Table 1 Summary of the device characteristics of white LECs

Device (**SR 101** concentration)	Bias (V)	CIE (x, y)[a]	CRI[a]	t_{max}[b] (min)	L_{max}[c] (cd m^{-2})	$\eta_{ext,max}$[d] (%)	$\eta_{p,max}$[e] (lm W^{-1})	$t_{1/2}$[f] (min)
I (0.3 wt%)	3.6 V	(0.32, 0.30)	72	90	12.6	7.5	13.7	120
	3.8 V	(0.30, 0.31)	73	60	19.4	7.9	15.6	90
II (0.5 wt%)	3.6 V	(0.33, 0.33)	79	90	7.2	7.3	13.5	170
	3.8 V	(0.31, 0.33)	76	70	8.0	7.5	14.2	170
III (0.8 wt%)	3.6 V	(0.31, 0.35)	78	150	2.2	6.9	14.2	200
	3.8 V	(0.31, 0.33)	77	130	2.9	6.9	14.3	180

[a] Evaluated from the EL spectra. [b] Time required to reach the maximal brightness. [c] Maximal brightness achieved at a constant bias voltage. [d] Maximal external quantum efficiency achieved at a constant bias voltage. [e] Maximal power efficiency achieved at a constant bias voltage. [f] The time for the brightness of the device to decay from the maximum to half of the maximum at a constant bias voltage.

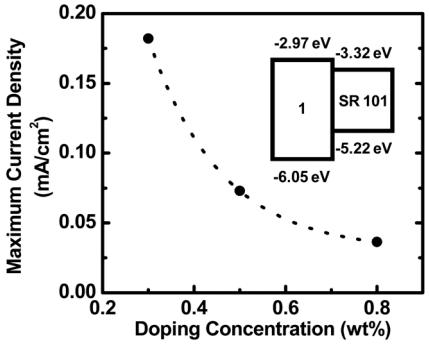

Fig. 5 Maximum current density *vs.* doping concentration characteristics for the white LECs containing **SR 101** of 0.3–0.5 wt%. Inset: the energy level diagram of the host (complex **1**) and the guest (**SR 101**) molecules.

Fig. 5. As the doping concentration of **SR 101** increases, charge trapping on the guest impedes carrier transport and the device current consequently decreases.

It is interesting to note that the full width at half maximum (FWHM) of the blue emission is much narrower in EL (Fig. 4) than that in PL (Fig. 3). To clarify such unusual phenomenon, optical simulation was performed to study the microcavity effect on the output EL spectrum of the white LECs. Since the optical thickness of the organic layer in the white LECs (320 nm) is comparable to the optical wavelength, the emission properties of organic materials can be modified in a microcavity structure, which alters the optical mode density within it and spectrally redistributes the EL spectrum. The output EL spectrum of a bottom emitting OLED device can be calculated approximately by using the following equation:[38]

$$|E_{\mathrm{ext}}(\lambda)|^2 = \frac{T_2 \frac{1}{N}\sum_{i=1}^{N}\left[1 + R_1 + 2\sqrt{R_1}\cos\left(\frac{4\pi z_i}{\lambda} + \varphi_1\right)\right]}{1 + R_1 R_2 - 2\sqrt{R_1 R_2}\cos\left(\frac{4\pi L}{\lambda} + \varphi_1 + \varphi_2\right)} \times |E_{\mathrm{int}}(\lambda)|^2$$

where R_1 and R_2 are the reflectances from the cathode and from the glass substrate, respectively, φ_1 and φ_2 are the phase changes on reflection from the cathode and from the glass substrate, respectively, T_2 is the transmittance from the glass substrate, L is the total optical thickness of the cavity layers, $|E_{\mathrm{int}}(\lambda)|^2$ is the emission spectrum of the organic materials without alternation of the microcavity effect, $|E_{\mathrm{ext}}(\lambda)|^2$ is the output emission spectrum from the glass substrate, z_i is the optical distance between the emitting sublayer i and the cathode. The emitting layer is divided into N sublayers and their contributions are summed up. Since the width of the p–n junction estimated by capacitance measurements was shown to be *ca.* 10% of the thickness of the emissive layer of LECs,[39] the emitting layer width of 32 nm and $N = 32$ was used in optical simulation. The PL spectra of thin films of complex **1** containing 0.3 wt% **SR 101** (Fig. 3) were used as the emission spectrum without alternation of the microcavity effect since no highly reflective metal layer is present in these samples. The simulation was implemented by using the MATLAB software. The simulated and measured output EL spectra of the white LECs with an emissive-layer thickness of 320 nm containing 0.3 wt% **SR 101** are shown in Fig. 6(a) for comparison. When the center of the emitting layer of the white LECs is set to be 195 nm away from the cathode, the simulated and measured output EL spectra match well. Such a position of the emitting layer is reasonable since a larger host–guest energy offset in the highest occupied molecular orbital (HOMO) level (inset of Fig. 5) results in more significant hole trapping and the recombination zone would be closer to the anode in consequence. Well-matched simulated and measured EL spectra of the white LECs confirm that reduced FWHM of the blue emission in EL results from destructive interference of the green part of the emission spectrum ($\lambda > 500$ nm) of complex **1**. If the thickness of the emissive layer is altered, the wavelength at which destructive interference occurs would be different and thus the output EL spectrum can be tailored. For instance, destructive interference of red emission takes place in the white LECs with an emissive-layer thickness of 270 nm (Fig. 6(b)). Simulation also predicts a similar result as compared to the experimental result (Fig. 6(b)). The tailoring output EL spectrum *via* the thickness dependent microcavity effect is especially useful for CTMC-based white LECs to achieve white EL with CIE coordinates approaching (0.33, 0.33) since saturated deep-blue emitting CTMCs have still been scarce up to now. The reported white LECs based on sky-blue emitting CTMCs generally exhibit greenish white EL even combined with saturated red CTMCs.[18,20,21,24] Without saturated deep-blue emitting CTMCs, suppressing green emission of sky-blue emitting CTMCs by employing the microcavity effect would be a feasible way to obtain more saturated blue emission and thus purer white EL emission.

The white LECs based on complex **1** doped with various **SR 101** concentrations and $BMIM^+(PF_6^-)$ (20 wt%) exhibited similar time-dependent EL characteristics under constant-bias operation. Fig. 7(a) and (b) show the time-dependent brightness/current density and EQE/power efficiency, respectively, at

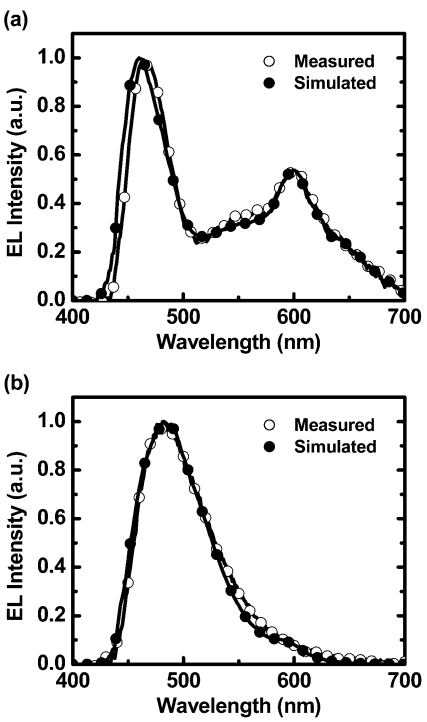

Fig. 6 Simulated and measured output EL spectra of the white LECs with emissive-layer thicknesses of (a) 320 nm and (b) 270 nm.

constant biases of 3.6 and 3.8 V for the white LECs with 0.3 wt% **SR 101** (Device I). After the bias was applied, the device current, brightness and device efficiency increased due to enhanced carrier injection induced by gradually formed p- and n-type doped layers near electrodes.[25] The brightness and device efficiency first increased with the device current and reached the maximum values. The peak EQE and the peak power efficiency at 3.6 and 3.8 V are (7.5% and 13.7 lm W^{-1}) and (7.9% and 15.6 lm W^{-1}), respectively. Then they dropped with time with a rate depending on the bias voltage (or current). The drop of brightness and device efficiency after reaching the peak value, as commonly seen in solid-state CTMC-based LECs,[6–32] may be associated with a few factors. When the device current is still increasing, the p- and n-type doped layers keep extending and the carrier injection efficiency is continuously enhanced. Therefore, the carrier recombination zone may keep moving closer to one electrode due to discrepancy in the enhancing rate of carrier injection efficiency, which would induce exciton quenching, deteriorating brightness and device efficiency.[40] The decrease in brightness and device efficiency at a relatively steady device current may be rationally attributed to the degradation of the emissive material during the LEC operation.[8] It is noted that unusual dips in brightness and device efficiency (valleys at *ca.* 150 and 100 min at 3.6 and 3.8 V, respectively) followed by a second rise were observed in the white LECs (Fig. 7(a) and (b)). A similar phenomenon was also reported in LECs based on relatively thicker (*ca.* 400 nm) neat films of complex **1** and was attributed to exciton quenching near the electrode due to the dynamic recombination zone during operation.[29] Initially, as the p- and n-type doped layers are gradually formed, the rate of enhancing injection efficiency of the hole would be faster than that of the electron since the required amount of accumulated anions near the anode for ohmic contact of holes would be less than the required amount of accumulated cations near the cathode for ohmic contact of electrons due to the lower injection barrier at the anode (see the inset of Fig. 5, work functions of PEDOT:PSS and Ag are 5.2 (ref. 41) and 4.26 eV (ref. 42), respectively). Excess holes would consequently push the recombination zone toward the cathode and exciton quenching would take place when the recombination zone is approaching the n-doped region, in which the ion density would be high.[43] Therefore, brightness and device efficiency of the white LECs would decrease at 90–150 and 60–100 min at 3.6 and 3.8 V, respectively (Fig. 7(a) and (b)). After the n-type doped region is well established, relatively balanced hole and electron injection would improve the balance of hole and electron densities in the emissive layer and thus the recombination zone would be pushed away from the n-doped region, resulting in recovering of brightness and device efficiency. The brightness and device efficiency of the white LECs deteriorate again after 200 and 130 min at 3.6 and 3.8 V, respectively, which would be attributed to degradation of the emissive material.[8] It is noted that no significant evolution in EL spectra has been observed during the time between two brightness maxima. As revealed in a previously reported model for operation of sandwiched LECs,[25] the thickness of the undoped region reduces rapidly after a bias is applied. The recombination zone would thus be confined in a relatively thinner undoped layer. A slight shift of the recombination zone due to alternation of carrier injection efficiency in a thin undoped layer would be sufficient to result in significant exciton quenching since the recombination zone is in close proximity of the doped regions.[40] However, the slight shift of the recombination zone in a relatively thinner undoped layer would not lead to significant difference in the optical distance between the emitting layer and the cathode, rendering a similar optical interference effect and thus no significant change in the EL spectra.

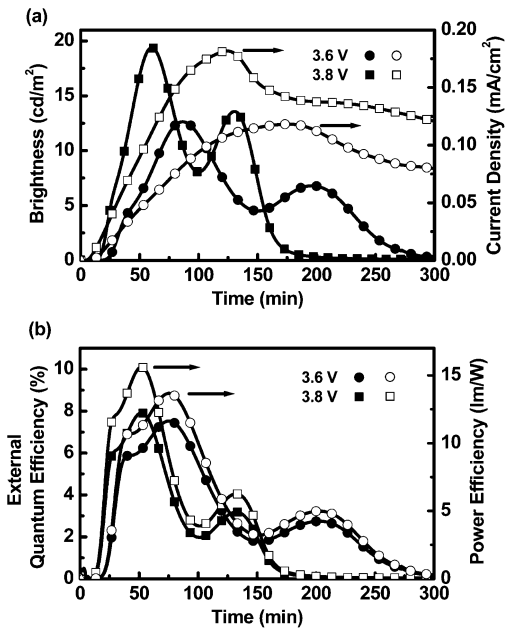

Fig. 7 (a) Brightness (solid symbols) and current density (open symbols) and (b) external quantum efficiency (solid symbols) and power efficiency (open symbols) as a function of time at a constant bias voltage of 3.6 and 3.8 V for the white LECs with 0.3 wt% **SR 101**.

The maximal EQE achieved from the phosphorescent sensitized white LECs (0.3 wt% **SR 101**) reached 7.9%, which is among the highest reported for white LECs and thus confirm that phosphorescent sensitization is useful for achieving efficient white LECs. However, the maximal EQE obtained is still lower than the value (*ca.* 14.4%) one could expect from a typical layered bottom-emitting all-phosphorescence device containing an emissive layer with a similar PLQY (0.72). Dexter energy transfer[44] and/or direct carrier trapping to form triplet excitons on guest molecules would be responsible for deteriorated device efficiency. Dexter energy transfer takes place between host triplets and guest triplets when the guest concentration increases, which would degrade the EL efficiency when occurring.[33] Direct carrier trapping results in formation of triplet excitons on guest molecules directly and would degrade device efficiency as well. Carrier trapping impedes carrier transport and thus lowers the device current of the host–guest LECs at the same bias voltage. Lowered device current with increasing doping concentration confirms direct carrier trapping (Fig. 5). Deteriorated device efficiencies of the white LECs doped with a higher guest concentration, which leads to more significant direct carrier trapping, also confirm direct formation of triplet excitons on the guests (Table 1). Furthermore, the carrier trapping effect has been shown to effectively tailor the carrier balance of single-layered LECs.[24,27,28] Carrier trapping induced by **SR 101** would also influence the carrier balance of complex **1**. Hence,

direct carrier trapping and modified carrier balance due to the large energy offsets between the energy levels of the host and the guest molecules (inset of Fig. 5) would play an important role in degradation of device efficiency of phosphorescent sensitized white LECs. Further studies of a host–guest system with appropriate energy level alignments to simultaneously suppress direct carrier trapping on the guest and to improve device carrier balance, *e.g.*, employing multiple guests,[24] may be beneficial for further enhancing of device efficiencies of phosphorescent sensitized white LECs. In addition, the enhancing device brightness would be another important issue for improving the performance of phosphorescent sensitized white LECs. The higher brightness of LECs has to be obtained at the expense of device stability.[7] To mitigate the device degradation and thus to obtain the best device efficiencies for clarifying the beneficial effect of adopting the phosphorescent sensitized strategy, the bias voltages of the white LECs were chosen to be relatively low (3.6 and 3.8 V). Better device efficiencies can generally be obtained at lower bias voltages (or current densities), as commonly observed in conventional OLEDs.[1,2] Therefore, operation of LECs at low biases is necessary to obtain good device efficiencies. Further studies for improving electrochemical stability of the host materials are still required to achieve high device efficiency at adequate brightness for practical applications.

Conclusions

In summary, we have demonstrated efficient phosphorescence sensitized white LECs based on a blue-emitting phosphorescent CTMC (complex **1**) doped with a red-emitting fluorescent dye (**SR 101**). Phosphorescence sensitized red fluorescence from an efficient red dye along with blue phosphorescence from a CTMC has been shown to provide efficient white EL emission. Maximal EQE and power efficiency of the phosphorescent sensitized white LECs reached 7.9% and 15.6 lm W^{-1}, respectively, which are among the highest reported for white LECs and confirm that phosphorescent sensitization is a useful technique for enhancing device efficiencies of white LECs. With the microcavity effect of the device structure, the green part of the EL spectrum of complex **1** can be suppressed due to destructive interference and more saturated blue EL emission can be obtained. Thus, white EL emission with CIE coordinates approaching (0.33, 0.33) can be achieved without employing saturated deep-blue emitting CTMCs.

Experimental

Photoluminescent characterization

The mixed films for PL studies were spin-coated at 3000 rpm onto quartz substrates (1 × 0.5 cm^2) using mixed solutions (in acetonitrile) of various ratios. The mass ratio of solute component of complex **1** and **SR 101** in acetonitrile solutions for spin coating of the mixed films is $(100 - x) : x$ ($x = 0.3$, 0.5 and 0.8). The concentrations of all solutions for spin coating are 150 mg mL^{-1}. The thickness of each spin-coated film was *ca.* 320 nm, as measured using ellipsometry. UV-Vis absorption spectra were recorded using a Hitachi U2800A spectrophotometer. PL spectra were recorded using a Hitachi F9500 fluorescence spectrophotometer. PLQYs for thin-film samples were determined with a calibrated integrating sphere system (HAMAMATSU C9920). The calculations of PLQYs were performed according to the reported literature:[45]

$$\eta = \frac{P_c - (1 - A)P_b}{L_a A}$$

where η is the PLQY, P_c is the PL intensity when the sample is in place and the excitation light beam is directed onto the sample, A is the fraction of the incident excitation light absorbed by the sample, P_b is the PL intensity when the sample is in place and the excitation light beam is directed onto the sphere wall and L_a is the intensity of the excitation light when the sphere is empty.

LEC device fabrication and characterization

ITO-coated glass substrates (2 × 2 cm^2) were cleaned and treated with UV/ozone prior to use. A PEDOT:PSS layer was spin-coated at 4000 rpm onto the ITO substrate in air and baked at 150 °C for 30 min. The emissive layer (~320 nm, as measured by ellipsometry) was then spin-coated at 3000 rpm from mixed acetonitrile solutions. The mass ratio of solute component of complex **1**, **SR 101** and $BMIM^+(PF_6^-)$ in acetonitrile solutions for spin coating of the mixed films is $(80 - x) : x : 20$ ($x = 0.3$, 0.5 and 0.8). The ionic liquid $[BMIM^+(PF_6)^-]$ was added to enhance the ionic conductivity of thin films and thus to reduce the turn-on time of the LEC device.[12] All solution preparing and spin-coating processes were carried out under ambient conditions. After spin coating, the thin films were then baked at 70 °C for 10 hours in a nitrogen glove box (oxygen and moisture levels below 1 ppm), followed by thermal evaporation of a 100 nm Ag top contact in a vacuum chamber (~10^{-6} torr). The electrical and emission characteristics of LEC devices were measured using a source-measurement unit and a Si photodiode calibrated with a Photo Research PR-650 spectroradiometer. All device measurements were performed at constant bias voltages (3.6 and 3.8 V). Since LEC devices deteriorate quickly in air and moisture, *i.e.*, the device lifetime ($t_{1/2}$) reduces to a few minutes, these devices were measured in a nitrogen glove box (oxygen and moisture level <1 ppm) to ensure stable operation. The EL spectra were taken with a calibrated CCD spectrograph.

Acknowledgements

The authors gratefully acknowledge the financial support from the National Science Council of Taiwan (NSC 101-2221-E-009-125).

References

1 J. Kido, K. Hongawa, K. Okuyama and K. Nagai, *Appl. Phys. Lett.*, 1994, **64**, 815.
2 Q. Pei, G. Yu, C. Zhang, Y. Yang and A. J. Heeger, *Science*, 1995, **269**, 1086.
3 Y. Yang and Q. Pei, *J. Appl. Phys.*, 1997, **81**, 3294.
4 M. Sun, C. Zhong, F. Li, Y. Cao and Q. Pei, *Macromolecules*, 2010, **43**, 1714.
5 S. Tang, J. Pan, H. Buchholz and L. Edman, *ACS Appl. Mater. Interfaces*, 2011, **3**, 3384.
6 J. K. Lee, D. S. Yoo, E. S. Handy and M. F. Rubner, *Appl. Phys. Lett.*, 1996, **69**, 1686.
7 H. Rudmann, S. Shimada and M. F. Rubner, *J. Am. Chem. Soc.*, 2002, **124**, 4918.

8 G. Kalyuzhny, M. Buda, J. McNeill, P. Barbara and A. J. Bard, *J. Am. Chem. Soc.*, 2003, **125**, 6272.
9 J. D. Slinker, D. Bernards, P. L. Houston, H. D. Abruña, S. Bernhard and G. G. Malliaras, *Chem. Commun.*, 2003, 2392.
10 H. Rudmann, S. Shimada and M. F. Rubner, *J. Appl. Phys.*, 2003, **94**, 115.
11 J. D. Slinker, A. A. Gorodetsky, M. S. Lowry, J. Wang, S. Parker, R. Rohl, S. Bernhard and G. G. Malliaras, *J. Am. Chem. Soc.*, 2004, **126**, 2763.
12 S. T. Parker, J. D. Slinker, M. S. Lowry, M. P. Cox, S. Bernhard and G. G. Malliaras, *Chem. Mater.*, 2005, **17**, 3187.
13 A. B. Tamayo, S. Garon, T. Sajoto, P. I. Djurovich, I. M. Tsyba, R. Bau and M. E. Thompson, *Inorg. Chem.*, 2005, **44**, 8723.
14 H. J. Bolink, L. Cappelli, E. Coronado, M. Grätzel and M. Nazeeruddin, *J. Am. Chem. Soc.*, 2006, **128**, 46.
15 H.-C. Su, F.-C. Fang, T.-Y. Hwu, H.-H. Hsieh, H.-F. Chen, G.-H. Lee, S.-M. Peng, K.-T. Wong and C.-C. Wu, *Adv. Funct. Mater.*, 2007, **17**, 1019.
16 H.-C. Su, C.-C. Wu, F.-C. Fang and K.-T. Wong, *Appl. Phys. Lett.*, 2006, **89**, 261118.
17 J. D. Slinker, J. Rivnay, J. S. Moskowitz, J. B. Parker, S. Bernhard, H. D. Abruña and G. G. Malliaras, *J. Mater. Chem.*, 2007, **17**, 2976.
18 H.-C. Su, H.-F. Chen, F.-C. Fang, C.-C. Liu, C.-C. Wu, K.-T. Wong, Y.-H. Liu and S.-M. Peng, *J. Am. Chem. Soc.*, 2008, **130**, 3413.
19 H.-C. Su, H.-F. Chen, C.-C. Wu and K.-T. Wong, *Chem.–Asian J.*, 2008, **3**, 1922.
20 L. He, J. Qiao, L. Duan, G. F. Dong, D. Q. Zhang, L. D. Wang and Y. Qiu, *Adv. Funct. Mater.*, 2009, **19**, 2950.
21 L. He, L. Duan, J. Qiao, G. Dong, L. Wang and Y. Qiu, *Chem. Mater.*, 2010, **22**, 3535.
22 M. Mydlak, C. Bizzarri, D. Hartmann, W. Sarfert, G. Schmid and L. De Cola, *Adv. Funct. Mater.*, 2010, **20**, 1812.
23 H.-C. Su, Y.-H. Lin, C.-H. Chang, H.-W. Lin, C.-C. Wu, F.-C. Fang, H.-F. Chen and K.-T. Wong, *J. Mater. Chem.*, 2010, **20**, 5521.
24 H.-C. Su, H.-F. Chen, Y.-C. Shen, C.-T. Liao and K.-T. Wong, *J. Mater. Chem.*, 2011, **21**, 9653.
25 M. Lenes, G. Garcia-Belmonte, D. Tordera, A. Pertegás, J. Bisquert and H. J. Bolink, *Adv. Funct. Mater.*, 2011, **21**, 1581.
26 C.-C. Ho, H.-F. Chen, Y.-C. Ho, C.-T. Liao, H.-C. Su and K.-T. Wong, *Phys. Chem. Chem. Phys.*, 2011, **13**, 17729.
27 C.-T. Liao, H.-F. Chen, H.-C. Su and K.-T. Wong, *J. Mater. Chem.*, 2011, **21**, 17855.
28 C.-T. Liao, H.-F. Chen, H.-C. Su and K.-T. Wong, *Phys. Chem. Chem. Phys.*, 2012, **14**, 1262.
29 H.-B. Wu, H.-F. Chen, C.-T. Liao, H.-C. Su and K.-T. Wong, *Org. Electron.*, 2012, **13**, 483.
30 C.-T. Liao, H.-F. Chen, H.-C. Su and K.-T. Wong, *Phys. Chem. Chem. Phys.*, 2012, **14**, 9774.
31 T. Hu, L. He, L. Duan and Y. Qiu, *J. Mater. Chem.*, 2012, **22**, 4206.
32 R. D. Costa, E. Ortí, H. J. Bolink, F. Monti, G. Accorsi and N. Armaroli, *Angew. Chem., Int. Ed.*, 2012, **51**, 8178.
33 M. A. Baldo, M. E. Thompson and S. R. Forrest, *Nature*, 2000, **403**, 750.
34 T. Förster, *Discuss. Faraday Soc.*, 1959, **27**, 7.
35 G. Lei, L. Wang and Y. Qiu, *Appl. Phys. Lett.*, 2004, **85**, 5403.
36 R. F. Kubin and A. N. Fletcher, *J. Lumin.*, 1982, **27**, 455.
37 R. A. Velapoldi and H. H. Tønnesen, *J. Fluoresc.*, 2004, **14**, 465.
38 X. Liu, D. Poitras, Y. Tao and C. Py, *J. Vac. Sci. Technol., A*, 2004, **22**, 764.
39 I. H. Campbell, D. L. Smith, C. J. Neef and J. P. Ferraris, *Appl. Phys. Lett.*, 1998, **72**, 2565.
40 K. W. Lee, J. D. Slinker, A. A. Gorodetsky, S. Flores-Torres, H. D. Abruña, P. L. Houston and G. G. Malliaras, *Phys. Chem. Chem. Phys.*, 2003, **5**, 2706.
41 Y. Shao, G. C. Bazan and A. J. Heeger, *Adv. Mater.*, 2007, **19**, 365.
42 A. A. Gorodetsky, S. Parker, J. D. Slinker, D. A. Bernards, M. H. Wong, G. G. Malliarasa, S. Flores-Torres and H. D. Abruña, *Appl. Phys. Lett.*, 2004, **84**, 807.
43 D. J. Dick, A. J. Heeger, Y. Yang and Q. Pei, *Adv. Mater.*, 1996, **8**, 985.
44 D. L. Dexter, *J. Chem. Phys.*, 1953, **21**, 836.
45 J. C. de Mello, H. F. Wittmann and R. H. Friend, *Adv. Mater.*, 1997, **9**, 230.

